Title	Investigation of the gut microbiome, bile acid composition and host immunoinflammatory response in a model of azoxymethane-induced colon cancer at discrete timepoints
Authors	Keane, Jonathan M.;Walsh, Calum J.;Cronin, P.;Baker, Kevin J.;Melgar, Silvia;Cotter, Paul D.;Joyce, Susan A.;Gahan, Cormac G. M.;Houston, Aileen M.;Hyland, Niall P.
Publication date	2022-11-23
Original Citation	Keane, J.M., Walsh, C.J., Cronin, P., Baker, K., Melgar, S., Cotter, P.D., Joyce, S.A., Gahan, C.G.M., Houston, A., and Hyland, N.P. (2022) 'Investigation of the gut microbiome, bile acid composition and host immunoinflammatory response in a model of azoxymethane-induced colon cancer at discrete timepoints', British Journal of Cancer, https://doi.org/10.1038/s41416-022-02062-4.
Type of publication	Article (peer-reviewed)
Link to publisher's version	https://doi.org/10.1038/s41416-022-02062-4 - 10.1038/s41416-022-02062-4
Rights	© The Author(s),This version of the article has been accepted for publication, after peer review and is subject to Springer Nature's AM terms of use, but is not the Version of Record and does not reflect post-acceptance improvements, or any corrections. The Version of Record is available online at: https://doi.org/10.1038/s41416-022-02062-4.
Download date	2024-03-29 12:05:43
Item downloaded from	https://hdl.handle.net/10468/13895

University College Cork, Ireland
Coláiste na hOllscoile Corcaigh

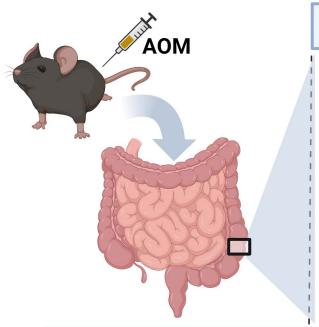

Progression following AOM

	Normal colon epithelium (week 8)	Normal colon epithelium (week 12)	Aberrant crypt foci (ACF) (week 24)	Adenoma (week 48)
	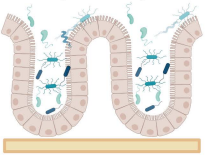	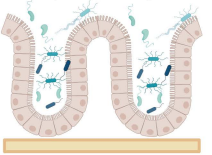	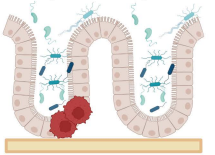	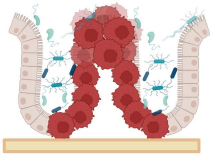
Microbiome	α-diversity ↑ Similarity ↓ Proteobacteria ↑	α-diversity ↔ Similarity ↓ Phyla ↔	α-diversity ↔ Similarity ↓ Phyla ↔	α-diversity ↔ Similarity ↓ Actinobacteria ↑ Verrucomicrobia ↓
Inflammation	No change	TNF-α ↑ CXCL1 ↑ IL-1β ↑ CXCL2 ↑ IL-12 ↑ CXCL5 ↑	IL-6 ↑ TNF-α ↑ IL-1β ↑ IL-12 ↑	No change
Bile Acids	Total ↓ 1^0 conjugated ↔ 1^0 unconjugated ↓ 2^0 conjugated ↓ 2^0 unconjugated ↓	Total ↓ 1^0 conjugated ↔ 1^0 unconjugated ↓ 2^0 conjugated ↔ 2^0 unconjugated ↓	Total ↔ 1^0 conjugated ↑ 1^0 unconjugated ↑ 2^0 conjugated ↑ 2^0 unconjugated ↓	No change

Investigation of the gut microbiome, bile acid composition and host immunoinflammatory response in a model of azoxymethane-induced colon cancer at discrete timepoints.

Keane JM [1, 2, 3, 4, 5], Walsh CJ [1, 6], Cronin P [1, 4], Baker K [3, 7], Melgar S [1], Cotter PD [1, 6], Joyce SA[*, 1, 4], Gahan CGM [*, 1, 2, 8], Houston A [*, 1, 3, #], Hyland NP [*, 1, 5].

1. APC Microbiome Ireland, University College Cork, Ireland
2. School of Microbiology, University College Cork, Ireland
3. Department of Medicine, University College Cork, Ireland
4. School of Biochemistry and Cell Biology, University College Cork, Ireland
5. Department of Physiology, University College Cork, Ireland
6. Teagasc Food Research Centre, Moorepark, Fermoy, Cork, Ireland
7. Department of Pathology, University College Cork, Ireland
8. School of Pharmacy, University College Cork, Ireland

*These authors contributed equally to this work

Corresponding Author

Clinical Science Building,

University College Cork,

Cork University Hospital,

Wilton,

Cork,

Ireland

Email: a.houston@ucc.ie; Dr Aileen Houston ORCiD (0000-0003-1362-5256)

Key words: Time-course, cytokine, chemokine, bile acids, tumorigenesis, microbiota

Abstract

Background: Distinct sets of microbes contribute to colorectal cancer (CRC) initiation and progression. Some occur due to the evolving intestinal environment but may not contribute to disease. In contrast, others may play an important role at particular times during the tumorigenic process. Here, we describe changes in the microbiota and host over the course of azoxymethane (AOM)-induced tumorigenesis. **Methods:** Mice were administered AOM or PBS and were euthanised 8, 12, 24 and 48 weeks later. Samples were analysed using 16S rRNA gene sequencing, UPLC-MS and qRT-PCR. **Results**: The microbiota and bile acid profile showed distinct changes at each timepoint. The inflammatory response became apparent at weeks 12 and 24. Moreover, significant correlations between individual taxa, cytokines and bile acids were detected. One co-abundance group (CAG) differed significantly between PBS- and AOM-treated mice at week 24. Correlation analysis also revealed significant associations between CAGs, bile acids and the bile acid transporter, ASBT. Aberrant crypt foci and adenomas were first detectable at weeks 24 and 48, respectively. **Conclusion:** The observed changes precede host hyperplastic transformation and may represent early therapeutic targets for the prevention or management of CRC at specific time-points in the tumorigenic process.

Introduction

Colorectal cancer (CRC) is the third most commonly diagnosed malignancy and the second leading cause of cancer-related death worldwide [1]. Most cases are sporadic in nature (approximately 75%) and occur in people without a genetic predisposition or a family history of CRC [2]. Recent studies have implicated the intestinal microbiome in the pathogenesis of CRC [3-5]. In healthy subjects, the gut is primarily populated by a core microbiota composed of obligate anaerobes belonging mainly to the phyla Firmicutes and Bacteroidetes, and to a lesser extent to Actinobacteria, Proteobacteria, and Verrucomicrobia [6]. Analysis of community diversity and richness indices based on 16S rRNA gene sequencing has shown significant alterations in microbial diversity both at the site of the primary tumour and in faecal samples from CRC patients [3, 7]. Understanding the role of the human gut microbiota in colon cancer, however, has largely depended on examining patients already presenting with CRC. To determine temporal changes in the gut microbiota at different stages of human colon cancer development, some studies have examined the microbiota profile in patients with intestinal polyps [8], with others examining the microbiota at different stages of the tumorigenic process [3, 5, 9]. Aberrant crypt foci (ACF) are thought to be the earliest identifiable lesion in the colon carcinogenic process [10], with microbiome changes associated with ACF recently identified in a human study [11]. The role of the gut microbiota in the progression from healthy to adenoma to CRC, however, is undoubtedly multifactorial and can affect the various stages of the tumorigenic process. This represents a significant challenge for human-based studies. Further research in experimental animal models is necessary to better understand the mechanisms that underlie the association between the gut microorganisms and CRC.

One mechanism by which the gut microbiota may affect colon carcinogenesis is the production or modification of metabolites such as bile acids [12]. Bile acids are endogenous, amphipathic molecules which facilitate uptake of dietary fats, and have been implicated in colon carcinogenesis [13]. For example, administration of cholic acid (CA), a primary bile acid, increased the incidence of colonic tumours in rats treated with genotoxic azoxymethane (AOM) [14]. In contrast, ursodeoxycholic acid (UDCA) reduced tumour burden [14], suggesting a dual role for bile acids in the tumorigenic process. Therefore, understanding the bile acid-gut microbiome axis in the development of colon cancer may reveal a dynamic mechanism by which the gut microbiota could influence cancer risk.

CRC-associated microbial communities also differentially correlate with the expression of host immunoinflammatory response genes [3]. Inflammation is a well characterised risk factor for CRC and a controlled inflammatory response is critical for immune protection against cancer [15]. Evidence suggests that the microbiota can influence colonic inflammation, and the microbiota is, in-turn, influenced by host inflammatory processes, resulting in complex reciprocal interactions [16, 17]. This is further supported by observations of microbial regulation of cytokines and chemokines in mouse models of CRC [18, 19]. Several cytokines, including interleukin 1β (IL-1β), interleukin 6 (IL-6) and tumour necrosis factor α (TNFα), have been shown to protect against cancer development in some circumstances, whilst contributing to tumour initiation and progression in others [20-22]. This highlights the importance of understanding the temporal expression profiles of these cytokines.

Here, we performed a time-course study in a C57BL/6J mouse strain with a prolonged period of disease onset following administration of AOM to establish the temporal sequence of events during tumorigenesis involving the microbiota, bile acid metabolism and expression of host immunoinflammatory genes. We identified distinct changes in both the immune and bile acid profiles, as well as particular microbial signatures that varied from the initial genotoxic insult to the appearance of pre-malignant disease and observed significant interactions between these factors.

Materials & Methods

Reagents

AOM (Merck, Darmstadt, Germany); RNAlater (Merck); Tetro cDNA synthesis kit (Bioline, Nottingham, UK); SensiFAST No-ROX kit (Bioline); QIAamp Fast DNA Stool Kit (Qiagen, Manchester, UK); nucleic acid probes from Roche Universal Probe Library; Custom oligo qPCR primers (Eurofins Genomics, Ebersberg, Germany).

Animals and Study Design

Animal experiments were conducted in accordance with the regulations and guidelines of the Irish Department of Health following approval by the University College Cork Animal Experimentation Ethics Committee (2011/023).

In this study, a total of 64 female C57BL/6JOlaHsd mice (6-8 weeks of age; Envigo, Blackthorne, UK) were housed in a specific pathogen-free facility on a 12-hour light/dark cycle at 22°C with access to water and chow *ad libitum*. After acclimatisation, equal numbers of mice were randomly assigned to two groups and were administered an intraperitoneal (i.p.) injection of 10mg/kg AOM to induce tumorigenesis (n = 32) each week for five consecutive weeks while control mice received phosphate buffer saline (PBS; n = 32). Following necropsy, each sample was allocated a random number, to which the subsequent investigators were blinded. To help to prevent horizontal microbiome transmission between co-housed mice, mice were group housed in two cages per treatment group (PBS or AOM) per cull time. Timed culls were performed at 8, 12, 24 and 48 weeks (n = 8 per group at each timepoint) following AOM or PBS administration and mice were euthanised by cervical dislocation. The experimental unit was considered a single animal. Sample size was calculated using g*power, with the standard deviation and magnitude of difference calculated from previous studies quantifying medium to large ACF development in response to AOM as an endpoint.

Faecal 16S rRNA Sequencing

DNA was extracted from faeces using the QIAamp Fast DNA Stool Kit as per the manufacturer's instructions with the addition of a bead-beating step.

The V3-V4 variable region of the 16S rRNA gene was amplified from each extracted DNA sample according to the 16S metagenomic sequencing library protocol (Illumina, San Diego, CA, USA) and sequenced on an Illumina MiSeq. See Methods in Supplementary Material.

Generating Co-abundance Groups

To identify patterns in the variation of the microbiota, a set of co-abundance groups (CAGs) were determined by clustering operational taxonomic units (OTUs) by the correlation of their relative abundances. Initially, OTUs were trimmed to remove taxa present in less than 20% of samples and all non-prokaryotic taxa. A matrix of Kendall's Tau values was then generated for each pair of OTUs, and these values were clustered by Ward-linkage according to their Pearson's correlation coefficient and visualised using the *Made4* package in R. Each cluster of taxa was then assigned to a CAG [23].

Ultra-Performance Liquid Chromatography – Mass Spectrometry (UPLS-MS)

Faecal samples were used for analysis of bile acids. UPLC-MS was performed as described [24]. Briefly, five microliters of extracted bile acids were injected onto a 50-mm T3 Acquity column and analysed in negative electrospray mode by an LCT Premier mass spectrometer (Waters, Dublin, Ireland). Each analyte was identified according to its mass and retention time. Standard curves were performed using known bile acids, and each analyte was quantified according to the standard curve and normalised according to the deuterated internal standards.

Cell Line Maintenance

HT29 cells were obtained from ATCC and maintained in DMEM supplemented with 10% foetal calf serum (FCS), and 1% penicillin/streptomycin solution in a 37°C, 5% CO_2 humidified incubator. Cells are routinely tested for mycoplasma contamination.

Faecal Water Preparation

Faecal water was prepared by suspending 0.3g faeces in 1mL PBS and subjected to bead beating for 15 seconds before centrifugation for 10 minutes. The supernatant was collected and stored at -20^{o}C before use. Faeces were pooled based on treatment and timepoint to generate sufficient material. HT29 cells were serum starved (0.5% FCS) overnight and were then exposed to faecal water (1:10 dilution) for four hours.

Quantitative Real-Time PCR

RNA extraction was performed using the GenElute Mammalian Total RNA kit (Merck) as per manufacturer instructions and converted to cDNA using the Tetro cDNA Synthesis Kit (Bioline). Genes were amplified using primers matched to appropriate hydrolysis probe from the Roche probe library (Supplemental Table 2) in a LightCycler 480 for 40 PCR cycles. Relative transcription was calculated using the $2^{-\Delta\Delta CT}$ method standardised to the average of the control group ΔCT [25]. Human CXCL1 was amplified using a primer-probe combination from Integrated DNA Technologies (Iowa, USA).

Statistics

Statistics were performed in SPSS Version 24 (Chicago, IL, USA), GraphPad version 9 (San Diego, CA, USA) and R Version 3.5.0 using the *Made4*, *vegan, pairwiseAdonis, compareGroups, phyloseq* and *ggplot* packages. Statistical significance was set to $p<0.05$. Benjamini-Hochberg FDR adjustment for multiple comparisons was applied where noted, with a false discovery rate set to 5%. Outliers were detected using Grubbs' test. Normality was determined by the Shapiro-Wilk test. Groups were compared by two-tailed student's t-test or MWU-test. Where the F value was statistically significant, data were analysed using the Welch t-test. For HT29 cell analysis, a one-tailed student's t-test was performed. Permutational ANOVA (PERMANOVA) was used to compare β-diversity and CAGs, using unweighted Unifrac and Euclidean-squared distance matrices, respectively. Correlations were examined using Pearson's R^2 and Spearman's R correlation coefficients. Throughout, asterisks denote significance where * represents $p<0.05$, ** $p<0.01$, and *** $p<0.001$.

Results

Macroscopic and microscopic changes in response to the carcinogen, AOM

Given that CRCs occur sporadically in most cases [2], we chose AOM alone to mimic human sporadic CRC development [26]. Moreover, as different mouse strains have been shown to exhibit differential sensitivity to AOM-induced tumorigenesis [26], we chose C57BL/6J mice, which display a lower sensitivity to AOM, to improve the temporal resolution of our study. Consistent with this approach, no signs of hyperplastic or neoplastic transformations were observed in mice at either 8- or 12-weeks post-AOM administration. Moreover, AOM-treated mice gained less weight than PBS-treated mice over the course of the study, and this difference in bodyweight-gain was significant at week 48 with AOM-treated mice weighing on average 3.4g less than PBS-treated mice (t-test, $p < 0.05$). Faecal occult blood (FOB) and ACF were first observed at week 24 (Table 1). FOB was also apparent in the faeces in three out of eight AOM-treated mice prior to week 48. Two of these mice harboured at least one colonic adenoma (Table 1).

Temporal microbiota changes in response to AOM

Shannon index (Figure 1a) was used to assess the α-diversity and evenness of gut microbiota in faecal samples from each experimental group. The observed species (OS; Figure 1a) index was used to estimate microbial richness, and the phylogenetic diversity (PD; Figure 1a) was also determined at each time-point. Analysis of AOM- versus PBS-treated mice revealed that the α-diversity of the microbiota was altered very early in the tumorigenic process. At week 8, OS and PD were significantly increased in AOM-treated mice (Figure 1a; MWU-test $p<0.05$ after FDR adjustment), suggesting that there is an increase in diversity within the AOM group at this time. Beta (β)-diversity (Figure 1b), which compares samples based on overall bacterial community composition across groups, also differed significantly between AOM- and PBS-treated mice at week 8 (Figure 1a; PERMANOVA of unweighted Unifrac, $p=0.008$, $R^2=0.153$). The dominant phyla in both AOM- and PBS-treated mice were Bacteroidetes and Firmicutes. Although the abundance of these phyla did not change significantly, we did observe a significant increase in Proteobacteria in AOM-treated mice (Figure 2a).

Of the significantly changed genera, the majority were among taxa corresponding to the Firmicutes, with changes also observed within Proteobacteria and Actinobacteria. At week 8, there was a significant suppression of *Lactobacillus* and an increase in *Olsenella* in AOM-

225 treated mice (Figure 3a; MWU-test, p<0.05 after FDR adjustment). Alterations in these taxa
226 have previously been correlated with colon cancer [27,28]. This decrease in *Lactobacillus* could
227 account for some of the changes observed in the bile acid pool at this time-point due to its
228 role in bile acid metabolism, although we did not observe any correlation between bile acids
229 and these bacterial genera. Since community structure can be more informative than
230 abundance differences of individual taxa, we next analysed the microbiota by determining
231 CAGs. The taxon composition of each CAG can be found in Supplemental Table 3. However,
232 we observed no significant difference between CAGs in either PBS- or AOM-treated groups
233 at week 8 (Figure 2b; t-test and MWU-test, p>0.05 after FDR adjustment).
234
235 At Week 12, there were no changes in α-diversity but β-diversity differed significantly
236 between treatments (Figure 1b; PERMANOVA of unweighted Unifrac distances, p=0.017,
237 R^2=0.149). At the phylum level, no alterations were detected (Figure 2a). There were only
238 nine individual genera that differed significantly between PBS- and AOM-treated mice
239 (Figure 3b). Moreover, as observed at week 8, there were no significant differences between
240 CAGs (Figure 2b; t-test and MWU-test, p>0.05 after FDR adjustment).
241
242 By week 24, no additional changes in α-diversity were observed (Figure 1a). However, β-
243 diversity differed significantly between AOM- and PBS-treated mice at weeks 24 and 48
244 (Figures 1b; PERMANOVA of unweighted Unifrac distances, p=0.001 and p=0.01,
245 respectively). Whilst there were no significant changes at the phylum level at week 24 (Figure
246 2a), changes were observed in specific members of Firmicutes, Bacteroidetes,
247 Proteobacteria and Tenericutes. Of the genera enriched in AOM-treated mice, *Oscillibacter*
248 was previously associated with increased cancer risk [3] (Figure 3c). At this time-point we
249 observed the first significant differences in the CAGs, with CAG5 being significantly
250 decreased in AOM-treated mice (Figure 2b; t-test, p<0.001 after FDR adjustment). This CAG
251 is dominated by Bacteroidetes which comprise >90% of its abundance.
252
253 At week 48, there was a significant increase in Actinobacteria and a significant reduction in
254 Verrucomicrobia in AOM-treated mice (Figure 2a). Of the significantly changed genera at this
255 time-point, *Akkermansia* was the only member of the Verrucomicrobia phylum that was
256 decreased (Figure 3d). Similarly, for Actinobacteria, *Bifidobacterium* was the only member of
257 this phylum that was increased. Moreover, at this time-point we observed the greatest

number of significantly altered genera (Figure 3d). These were predominantly Firmicutes (7/21), Proteobacteria (5/21) and Tenericutes (5/21).

Bile acid metabolism following AOM administration

Dysregulation of bile acids has been implicated in tumorigenesis [13]. Bile that is not re-absorbed in the small intestine is subjected to microbial transformation. First, bile salts are deconjugated from taurine and glycine by the bacterial enzyme bile salt hydrolases (*bsh*) to form free bile acids. Unconjugated primary bile acids (mainly cholic acid (CA), chenodeoxycholic acid (CDCA) and muricholic acid (MCA) in mice) are converted into secondary bile acids, such as deoxycholic acid (DCA), lithocholic acid (LCA), and ursodeoxycholic acid (UDCA) by bacterial 7α-dehydroxylase. Moreover, the apical sodium-dependent bile acid transporter (ASBT) is expressed on the apical membrane of enterocytes and mediates the reabsorption of bile acids from the intestine. With respect to the faecal bile acid analysis, the concentration of total bile acids was significantly reduced in AOM-treated mice at week 8 (Figure 4a; t-test, $p<0.01$). Both unconjugated primary (CDCA) and conjugated and unconjugated secondary bile acids (DCA, LCA, T-LCA) were also reduced at this time (Figure 4c). Interestingly, the proportion of the hydrophobic cytotoxic bile acids, DCA and LCA (Figure 4c; t-test, $p<0.001$ after FDR adjustment), were significantly decreased in the faeces of AOM-treated mice at week 8.

The total amount of bile acids in the faeces, as well as the levels of DCA and LCA remained significantly reduced at week 12 (Figures 4a and d; t-test, $p<0.001$ after FDR adjustment). This agrees with previous work which demonstrated a similar pattern for LCA and DCA in a colitis-associated model of colon cancer [29]. Moreover, faecal waters from patients with colon cancer had decreased levels of DCA, LCA and cholate relative to healthy controls [30].

The concentrations of primary unconjugated (CDCA, β-MCA) and conjugated (T-CA, T-β-MCA) faecal bile acids were increased in AOM-treated mice at week 24, of which β-MCA was the most abundant (Figure 4e; t-test, $p<0.05$ after FDR adjustment). There was also an increase in both taurine-conjugated primary and secondary bile acids. In contrast, LCA was significantly reduced (Figure 4e; t-test, $p<0.05$ after FDR adjustment). Moreover, expression of *ASBT* was significantly reduced (t-test, $p<0.01$). By week 48, there was no significant change in the bile acid profile (Figure 4a and 4f).

291

292 *Colonic inflammatory response to AOM*

293 Given that inflammation is a risk factor for colon cancer and can influence colon
294 carcinogenesis, we measured the transcription of several cytokines and chemokines in the
295 distal large intestine (Figure 5a). Significant increases in cytokine and chemokine expression
296 patterns become apparent at week 12, with the expression of *TNFα*, *IL-1β*, *IL-12*, *CXCL1*,
297 *CXCL2* and *CXCL5* significantly up-regulated in AOM-treated mice (Figure 5; t-test, $p<0.05$,
298 $p<0.01$, $p<0.001$ after FDR correction). *TNFα* remained elevated at week 24, together with
299 an increase in gene expression of *IL-6*, *IL-1β* and *IL-12* (Figure 5a; t-test, $p<0.05$ after FDR
300 correction). However, these alterations in cytokine and chemokine transcription were absent
301 by week 48. Consistent with these findings, human colonic tumour cells display a similar
302 temporal response following stimulation with faecal waters isolated from AOM-treated mice
303 relative to PBS-treated mice at the same time-points. At weeks 12 and 24, *CXCL2* and *CXCL1*
304 were significantly increased in the HT29 cells, respectively. In this human cell line, the
305 changes in immunoregulatory gene expression were also increased following stimulation
306 with faecal water prepared from week 48, but these changes were not significant.

307

308 *Correlation analyses between the gut microbiota and immunoinflammatory cytokines and*
309 *bile acid composition*

310 Correlation analyses were performed to identify any relationships between the microbiome,
311 cytokine transcription and the bile acid pool. At week 8, *Allobaculum* negatively correlated
312 with *IL-12* (Spearman, $p<0.001$, $R=-1$), *Coriobacteriaceae_uncultured* negatively correlated
313 with *CXCL1* and *IL-6* ($p<0.001$, $R=-0.97$; $p<0.001$, $R=-0.95$, respectively) and
314 *Defluviitaleaceae_uncultured* negatively correlated with *IL-1β* (Spearman, $p<0.001$, $R=-0.95$).
315 No additional correlations between individual taxa and cytokines were observed at any other
316 time-point in AOM-treated mice. At weeks 12 and 24, we observed significant correlations
317 between bile acids and individual taxa (Supplemental Table 4). With the exception of
318 *Parasutterella* which positively correlated with T-UDCA (Spearman, $p<0.001$, $R=1$), all other
319 correlations were negative (Supplemental Table 4). We also investigated whether any
320 correlations existed between CAGs, inflammatory genes, bile acids, and *ASBT* expression.
321 CAG2 negatively correlated with DCA at week 24 (Spearman, $p<0.001$, $R=-1$). At week 48,
322 CAG4 (Spearman, $p<0.001$, $R=0.952$) and CAG5 (Spearman, $p<0.01$, $R=0.81$) positively
323 correlated with *ASBT* expression, whilst CAG8 negatively correlated (Spearman, $p<0.05$, $R=-$
324 0.857).

Discussion

Decreased α-diversity in the faecal microbiome has been described as a characteristic feature of CRC [7, 31]. However, studies have also reported an increase in α-diversity in patients with colon cancer [32, 33]. This divergence may be associated with the stage of the disease [31]. In support of this, our data suggest that carcinogenesis begins with an increase in α-diversity as characterised by an increase in PD and observed species in AOM-treated mice at week 8. This suggests that there are more OTUs present in the AOM group which are further away from each other on the phylogenetic tree. The presence of a small number of highly divergent OTUs would greatly impact PD without having a major impact on richness. When considering which taxa might account for the increase in PD but not richness, we identified multiple taxa which were either present in one treatment group and absent in the other or *vice versa* at week 8. Most of these OTUs fell within the phyla Bacteroidetes (uncultured), Firmicutes (e.g. *Erysipelotrichaceae*, *Roseburia*, *Blautia*) or Tenericutes (*Mollicutes*). From week 12 onward, this change in α-diversity was no longer apparent. However, by week 12, a significant up-regulation of pro-inflammatory signalling was detected in mice administered AOM. At this time-point, the microbial communities became more similar, and one possible explanation may be that the increase in α-diversity observed early in the tumorigenic process is due to the growth of opportunistic pathogens and is reversed later once the immune response becomes more active.

In this context, the opportunistic pathogen *Clostridium sensu stricto*, which was decreased at week 8 in our study, and then increased at week 12, occurred at a time where the inflammatory response also significantly changed in our mouse model of colon carcinogenesis. A similar positive relationship between this taxon and inflammation was shown in a mouse model of inflammatory bowel disease (IBD) [34]. Other taxa that changed over time included *Turicibacter*, which was decreased at week 8 but increased at week 48 in our model. Whilst little is known about a direct role for this genus in inflammation and colorectal cancer, its abundance was previously found to be decreased in TNFα-deficient mice compared to wildtype mice [35]. Other studies have also suggested that this genus benefits from a pro-inflammatory environment which is consistent with the absence of an overt inflammatory response in our model at week 8 [36]. Finally, *Marvinbryantia*, with the exception of week 12, was significantly decreased over time. This genus has also been shown to be reduced in CRC [37]. Moreover, in a rat model of colitis, *Marvinbryantia* was significantly increased in response to feeding with resistant starch. This was associated with decreased

tumour multiplicity, increased short chain fatty acid production and reduced proliferation and inflammation, suggesting that it may have anti-inflammatory and protective properties [38]. These data reflect the dynamic interplay between inflammation and the microbiome and suggest that temporal changes in the abundance of specific genera may be dependent on the host inflammatory response at particular time-points during the course of tumorigenesis.

Turicibacter, the second most abundant member of CAG5, correlates with the activity of *Slc10a2*, which encodes ASBT and helps recycle bile acids from the small intestine back to the liver [39]. Moreover, expression of ASBT is sensitive to changes in the microbiome [40]. We observed that ASBT expression tended to follow a similar dynamic pattern over time as total bile acids, but there was no significant correlation after FDR correction between the expression of this transporter and the bile acids measured. However, of the 12 faecal bile acids measured, eight were significantly increased when expression of ASBT was significantly decreased, in particular conjugated bile acids that have high substrate specificity for this transporter [41]. This in turn could potentially lead to increased luminal concentrations of the farnesoid X receptor (FXR) antagonist, T-βMCA, which is normally transported by ASBT, and this, coupled with an increase in the ASBT-independent transport of the FXR agonist, CDCA, may potentially influence tumorigenesis through alterations in FXR signalling.

The presence of high levels of bile acids also suppresses the activity of *Turicibacter* [39]. Moreover, studies examining the effect of *Turicibacter sanguinis* on bile acid metabolism and transformation suggest that this human isolate can de-conjugate T-CA and transform CA and CDCA by the action of the microbial bile acid-metabolising enzyme 7α-hydroxysteroid dehydrogenase [39]. Therefore, fluctuations in the abundance of this taxon over time might not only affect bile acid metabolism, but the bile acid profile at any given time-point could also influence the abundance of *Turicibacter*. The next most abundant members of CAG5 are *Parasutterella* and *Bifidobacterium*. Of these, *Bifidobacterium* display sensitivity to fluctuations in bile acids, in particular to the toxic effects of the secondary bile acids such as DCA [42]. Moreover, colonisation with *Parasutterella* modified the bile acid metabolites, thereby impacting bile acid transport and synthesis [43]. Taken together, these findings suggest that significant changes in the relative abundance of individual taxa responsible for bile acid metabolism and modification may not necessarily be reflected in the expected faecal bile acid profile, or *vice versa*, particularly in the context of a more complex ecosystem in which

members not only metabolise bile acids but are also sensitive to their growth inhibitory effects.

The only correlation between CAGs and bile acids was between the secondary bile acid, DCA and CAG2 and this occurred at week 24. DCA also significantly correlated with *Bacteriodes* at this time-point. DCA has been shown to be toxic and inhibit the growth of *Bacteriodes* [44]. However, we observed no significant difference in either this taxon or in the faecal levels of DCA at this time-point. This taxon is also the most abundant member of CAG2, which, in turn, was also negatively associated with DCA. Whilst the relative abundance of the taxon within the CAG did not change, another member of this CAG, *Bacteroidales S24-7*, showed a five-fold reduction in AOM-treated mice relative to control mice. Moreover, this taxon was significantly less abundant in AOM-treated mice at this time-point (see Figure 3). *Bacteroidales S24-7* has previously been shown to positively correlate with caecal levels of T-DCA in a mouse model of liver regeneration [45]. Of note, levels of *Bacteroidales* have been shown to be significantly reduced in patients with CRC relative to healthy controls [46].

Expression of the bile acid transporter ASBT positively correlated with CAG5 at week 48. At this time-point the abundance of *Bifidobacterium* also significantly increased in AOM-treated mice (see Figure 3). Moreover, within CAG5, the abundance of this taxon increased three-fold. Bifidobacteria have bile acid-deconjugating activity which is consistent with the normalisation of conjugated bile acids at week 48, relative to week 24, when the abundance of this species significantly increased. Notably, expression of the bile acid receptor FXR is down-regulated in human colorectal tumours and colon cancer cell lines [47]. Moreover, administration of tauro-conjugated β-MCA, which is an FXR antagonist, accelerated tumour growth and increased the serum levels of pro-inflammatory cytokines in APC^{MIN} mice [48]. Given the ability of bifidobacteria, which are significantly more abundant at week 48, to deconjugate the endogenous FXR antagonist T-β-MCA and relieve its FXR antagonism in mice, this is consistent with a possibly pro-tumorigenic effect of T-β-MCA and FXR 24 weeks after AOM administration.

CAG4 also positively correlated with ASBT expression at week 48. Although the most abundant taxon within CAG4 was *Bacteroidales S24- 7*, this was comparable within the CAG for PBS- and AOM-treated mice. However, *Akkermansia*, the second most abundant taxon within this CAG, differed between treatments both at the taxon level (see Figure 3) and

within CAG4 (approx. 2.5-fold reduction in AOM treated mice). *A. muciniphila* is one of the most studied species of this genus and displays sensitivity to several bile salts [49], further highlighting the complexity and inter-relationship between bacterial metabolites and the composition of the microbiome. We also observed a negative correlation between the phylum to which this genus belongs, Verrucomicrobia and the genus itself at weeks 12 and 24 with UDCA, and T-CA and T-UDCA respectively. Studies have demonstrated that these bile acids do not affect the growth of *A. muciniphila* [49], suggesting that this relationship may be driven by other members of this phylum.

In contrast, CAG8 negatively correlated with ASBT expression at week 48. The most abundant members of CAG8 are *Blautia, Ruminococcaceae_uncultured* and *Lachnospiraceae*, which have all been associated with secondary bile acids and bile acid deconjugation [50, 51]. Of these three taxa, only the abundance of *Lachnospiraceae* in CAG8 was differentially altered between PBS- and AOM-treated mice (1.5-fold reduction). Moreover, members of the *Lachnospiraceae* family negatively correlated with CDCA in IBD [52]. However, in a model of liver regeneration no relationship between either individual caecal bile acids or ASBT was observed with *Lachnospiraceae* [45]. Despite the bile acid metabolising activity of this taxon, we did not observe any significant relationship between *Lachnospiraceae* and individual bile acids. Moreover, the decrease in abundance is consistent with observations that this taxon is significantly reduced in the gut of individuals with CRC [46]. Given that ASBT expression and faecal bile acid profile had normalised at week 48 in our study, the role of this CAG in bile acid transport and metabolism respectively is unclear.

Of the genera that correlated with inflammatory gene expression, these occurred at week 8 when there was no obvious change in inflammation. Of note, *Allobaculum* negatively correlated with the expression of IL-12. Little is known about *Allobaculum*, although studies have shown that it is increased in IBD [53] and with Th 17 cell activity [54], suggesting that this taxon may be pro-inflammatory. IL-6, IL-1β, and CXCL1 have all been linked to colon carcinogenesis and at week 8, both IL-6 and CXCL1 negatively correlated with *Coriobacteriaceae*, whilst *Defluviitaleaceae* negatively correlated with IL-1β. Despite these correlations, however, the only significant alterations in inflammatory gene expression occurred at weeks 12 and 24. Previous studies have proposed that particular bacterial clusters or CAGs may be more important in colon tumorigenesis than individual taxa [3]. It could be argued in our study that CAG1 is pathogenic, given that it contains *Citrobacter* [55],

460 *Hydrogenoanaerobacterium* [56], and *Anaeroplasma* [57] which have been associated with colon
461 cancer. However, the most abundant member of this CAG belongs to the uncultured
462 *Clostridium vadinBB60 group*, and therefore we could not definitively classify this CAG as
463 pathogenic or pro-inflammatory.
464
465 Although we observed significant changes in both inflammatory factors and bile acids very
466 early on in the tumorigenic process, few correlations were detected between these factors.
467 However, there are other microbial drivers that could influence colonic tumorigenesis. For
468 instance, gut-microbiota-derived metabolites such as hydrogen sulphide and N-nitroso
469 compounds have been implicated in CRC [58]. Moreover, oxidative stress and reactive oxygen
470 species have also been linked to CRC [59]. Indeed, continuous exposure of intestinal epithelial
471 cells to high concentrations of secondary bile acids has been shown to induce the production
472 of reactive oxygen species and active nitrogen species [60]. However, given that we observed
473 a significant decrease in DCA and LCA early in response to AOM, we can only speculate on
474 the contribution of bile acid-induced ROS generation early in the tumorigenic process.
475
476 Early changes in the microbiome or microbiome-associated metabolites could potentially
477 represent early biomarkers for CRC development. A recent human study has examined the
478 microbiome of ACF and ACF with synchronous polyps which likely reflects some of the
479 earliest changes in the microbiome [11]. When these human samples were stratified by the
480 presence of ACF alone versus those with ACF and polyp, two distinct microbial clusters were
481 apparent, with compositional changes in Firmicutes predominating [11]. Of the significantly
482 changed phyla at weeks 24 and 48 in our study, the majority also occurred within the
483 Firmicutes phylum. Furthermore, in taxon-based analysis, the microbiota profile from
484 patients with conventional adenomas was depleted in a network of Clostridia OTUs from
485 families *Ruminococcaceae*, *Clostridiaceae*, and *Lachnospiraceae* [61]. Whilst we also saw
486 significant changes in Clostridia OTUs from these families, these were divergent, with
487 increases and decreases in abundance seen. Our study identifies early changes in the
488 microbiome prior to tumour development and likely reflects the equivalent premalignant
489 lesions (ACF and adenoma) in human studies.
490
491 Most of the significant changes in phyla occurred at week 48 and was characterised by a
492 significant reduction in Verrucomicrobia and an increase in Actinobacteria. This reduction in
493 Verrucomicrobia, if sustained, could be associated with improved outcome as a decrease in

this phylum is associated with a reduction in tumour development, invasiveness, and inflammation in a mouse model of colon cancer [62, 63]. However, the alterations in Actinobacteria observed in our study do not appear to be reflected in human disease and therefore Actinobacteria is unlikely to reflect a pre-cancerous biomarker for CRC in human studies [64, 65]. Moreover, bile acids were also investigated for their potential as microbiome-associated biomarkers for the development of CRC [66], but the findings were unclear. Discrete taxonomic changes were also observed in our study which may reflect potential beneficial pre-malignant microbiome biomarker. The composition of the microbiome has also been implicated in treatment response. For example, Vibrio and Psychrobacter, both of which are Gammaproteobacteria, were significantly reduced at all four time points in our study. Notably the presence of intra-tumoral Gammaproteobacteria in pancreatic cancer resulted in treatment resistance to the chemotherapeutic, gemcitabine [67]. Whether the changes in the faecal microbiome represent prognostic or predictive biomarkers for disease for treatment response warrants further investigation in CRC.

In conclusion, the first changes we observed in response to AOM treatment were microbial in nature, potentially pro-tumorigenic, and preceded inflammatory changes in the host. Concurrent alterations in the bile acid pool, possibly reflecting a reduction in microbial bile acid metabolism, were also significant in the earlier phase following AOM treatment. Whilst a significant cytokine response ensued, this was largely ameliorated by week 48 when macroscopic adenomas appeared. Our study highlights the complexity of microbe-host interactions in the pathogenesis of colon cancer and the discrete events which occur following a genotoxic insult. Improved understanding of these interactions could lead to better interventional strategies to suppress the development of colon cancer at key stages in the tumorigenic process.

Additional Information

Acknowledgements

We acknowledge Pat Casey for his assistance with the animal studies. Graphical abstract was created with BioRender.com.

Data Availability Statement

The data underlying this article will be shared on a reasonable request to the corresponding author.

Authors' contributions

JMK acquired data, and played an important role in interpreting the results and drafted the manuscript. CJW, PC and KB acquired data. SM helped to design the work that led to the submission. PDC helped draft the manuscript, acquired data, and/or played an important role in interpreting the results. SAJ, CGMG, AH and NPH conceived and designed the work that led to the submission, played an important role in interpreting the results, and drafted the manuscript. All authors approved the final version and agreed to be accountable for all aspects of the work.

Ethics approval

Animal experiments were conducted in accordance with the regulations and guidelines of the Irish Department of Health following approval by the University College Cork Animal Experimentation Ethics Committee (2011/023).

Data availability

The datasets generated and/or analysed during the current study are available from the corresponding author on reasonable request.

Competing interests

The authors are not aware of any competing interests that might be perceived as affecting the findings of this study.

Funding information

This work was supported by the APC Innovation Platform. APC Microbiome Ireland is a research institute funded by Science Foundation Ireland (SFI) through the Irish Governments National Development Plan (Grant SFI/12/RC/2273).

553 **References**

554 1. Keum N, Giovannucci E. Global burden of colorectal cancer: emerging trends, risk
555 factors and prevention strategies. Nat Rev Gastroenterol Hepatol. 2019;16(12):713-32.
556 2. Yamagishi H, Kuroda H, Imai Y, Hiraishi H. Molecular pathogenesis of sporadic
557 colorectal cancers. Chin J Cancer. 2016;35:4.
558 3. Flemer B, Lynch DB, Brown JM, Jeffery IB, Ryan FJ, Claesson MJ, et al. Tumour-
559 associated and non-tumour-associated microbiota in colorectal cancer. Gut. 2017;66(4):633-
560 43.
561 4. Scott AJ, Alexander JL, Merrifield CA, Cunningham D, Jobin C, Brown R, et al.
562 International Cancer Microbiome Consortium consensus statement on the role of the human
563 microbiome in carcinogenesis. Gut. 2019;68(9):1624-32.
564 5. Dulal S, Keku TO. Gut microbiome and colorectal adenomas. Cancer J.
565 2014;20(3):225-31.
566 6. Eckburg PB, Bik EM, Bernstein CN, Purdom E, Dethlefsen L, Sargent M, et al. Diversity
567 of the human intestinal microbial flora. Science. 2005;308(5728):1635-8.
568 7. Ahn J, Sinha R, Pei Z, Dominianni C, Wu J, Shi J, et al. Human gut microbiome and risk
569 for colorectal cancer. Journal of the National Cancer Institute. 2013;105(24):1907-11.
570 8. Mangifesta M, Mancabelli L, Milani C, Gaiani F, de'Angelis N, de'Angelis GL, et al.
571 Mucosal microbiota of intestinal polyps reveals putative biomarkers of colorectal cancer. Sci
572 Rep. 2018;8(1):13974.
573 9. Ohigashi S, Sudo K, Kobayashi D, Takahashi O, Takahashi T, Asahara T, et al. Changes
574 of the intestinal microbiota, short chain fatty acids, and fecal pH in patients with colorectal
575 cancer. Dig Dis Sci. 2013;58(6):1717-26.
576 10. Alrawi SJ, Schiff M, Carroll RE, Dayton M, Gibbs JF, Kulavlat M, et al. Aberrant crypt
577 foci. Anticancer Res. 2006;26(1a):107-19.
578 11. Hong BY, Ideta T, Lemos BS, Igarashi Y, Tan Y, DiSiena M, et al. Characterization of
579 Mucosal Dysbiosis of Early Colonic Neoplasia. NPJ Precis Oncol. 2019;3:29.
580 12. Keane JM, Joyce SA, Gahan CGM, Hyland NP, Houston A. Microbial Metabolites as
581 Molecular Mediators of Host-Microbe Symbiosis in Colorectal Cancer. Results Probl Cell
582 Differ. 2020;69:581-603.
583 13. Ocvirk S, O'Keefe SJ. Influence of Bile Acids on Colorectal Cancer Risk: Potential
584 Mechanisms Mediated by Diet - Gut Microbiota Interactions. Curr Nutr Rep. 2017;6(4):315-
585 22.
586 14. Earnest DL, Holubec H, Wali RK, Jolley CS, Bissonette M, Bhattacharyya AK, et al.
587 Chemoprevention of azoxymethane-induced colonic carcinogenesis by supplemental dietary
588 ursodeoxycholic acid. Cancer Res. 1994;54(19):5071-4.
589 15. Adam JK, Odhav B, Bhoola KD. Immune responses in cancer. Pharmacol Ther.
590 2003;99(1):113-32.
591 16. Zuo T, Ng SC. The Gut Microbiota in the Pathogenesis and Therapeutics of
592 Inflammatory Bowel Disease. Front Microbiol. 2018;9:2247-.
593 17. Arthur JC, Perez-Chanona E, Mühlbauer M, Tomkovich S, Uronis JM, Fan T-J, et al.
594 Intestinal inflammation targets cancer-inducing activity of the microbiota. Science.
595 2012;338(6103):120-3.
596 18. Lucas C, Barnich N, Nguyen HTT. Microbiota, Inflammation and Colorectal Cancer.
597 Int J Mol Sci. 2017;18(6):1310.
598 19. Mendes MCS, Paulino DSM, Brambilla SR, Camargo JA, Persinoti GF, Carvalheira JBC.
599 Microbiota modification by probiotic supplementation reduces colitis associated colon
600 cancer in mice. World J Gastroenterol. 2018;24(18):1995-2008.
601 20. Bent R, Moll L, Grabbe S, Bros M. Interleukin-1 Beta-A Friend or Foe in Malignancies?
602 Int J Mol Sci. 2018;19(8).

21. Scheller J, Chalaris A, Schmidt-Arras D, Rose-John S. The pro- and anti-inflammatory properties of the cytokine interleukin-6. Biochim Biophys Acta. 2011;1813(5):878-88.
22. Wang X, Lin Y. Tumor necrosis factor and cancer, buddies or foes? Acta Pharmacol Sin. 2008;29(11):1275-88.
23. Claesson MJ, Jeffery IB, Conde S, Power SE, O'Connor EM, Cusack S, et al. Gut microbiota composition correlates with diet and health in the elderly. Nature. 2012;488(7410):178-84.
24. Joyce SA, MacSharry J, Casey PG, Kinsella M, Murphy EF, Shanahan F, et al. Regulation of host weight gain and lipid metabolism by bacterial bile acid modification in the gut. Proceedings of the National Academy of Sciences. 2014;111(20):7421-6.
25. Livak KJ, Schmittgen TD. Analysis of relative gene expression data using real-time quantitative PCR and the 2(-Delta Delta C(T)) Method. Methods (San Diego, Calif). 2001;25(4):402-8.
26. Rosenberg DW, Giardina C, Tanaka T. Mouse models for the study of colon carcinogenesis. Carcinogenesis. 2009;30(2):183-96.
27. Chen W, Liu F, Ling Z, Tong X, Xiang C. Human intestinal lumen and mucosa-associated microbiota in patients with colorectal cancer. PLoS One. 2012;7(6):e39743.
28. Fang CY, Chen JS, Hsu BM, Hussain B, Rathod J, Lee KH. Colorectal Cancer Stage-Specific Fecal Bacterial Community Fingerprinting of the Taiwanese Population and Underpinning of Potential Taxonomic Biomarkers. Microorganisms. 2021;9(8).
29. Liu L, Yang M, Dong W, Liu T, Song X, Gu Y, et al. Gut Dysbiosis and Abnormal Bile Acid Metabolism in Colitis-Associated Cancer. Gastroenterol Res Pract. 2021;2021:6645970.
30. Le Gall G, Guttula K, Kellingray L, Tett AJ, Ten Hoopen R, Kemsley EK, et al. Metabolite quantification of faecal extracts from colorectal cancer patients and healthy controls. Oncotarget. 2018;9(70):33278-89.
31. Ai D, Pan H, Li X, Gao Y, Liu G, Xia LC. Identifying Gut Microbiota Associated With Colorectal Cancer Using a Zero-Inflated Lognormal Model. Front Microbiol. 2019;10(826).
32. Feng Q, Liang S, Jia H, Stadlmayr A, Tang L, Lan Z, et al. Gut microbiome development along the colorectal adenoma–carcinoma sequence. Nature Communications. 2015;6:6528.
33. Scanlan PD, Shanahan F, Clune Y, Collins JK, O'Sullivan GC, O'Riordan M, et al. Culture-independent analysis of the gut microbiota in colorectal cancer and polyposis. Environmental microbiology. 2008;10(3):789-98.
34. Zou J, Shen Y, Chen M, Zhang Z, Xiao S, Liu C, et al. Lizhong decoction ameliorates ulcerative colitis in mice via modulating gut microbiota and its metabolites. Applied Microbiology and Biotechnology. 2020;104(13):5999-6012.
35. Jones-Hall YL, Kozik A, Nakatsu C. Ablation of tumor necrosis factor is associated with decreased inflammation and alterations of the microbiota in a mouse model of inflammatory bowel disease. PLoS One. 2015;10(3):e0119441.
36. Rausch P, Steck N, Suwandi A, Seidel JA, Künzel S, Bhullar K, et al. Expression of the Blood-Group-Related Gene B4galnt2 Alters Susceptibility to Salmonella Infection. PLoS Pathog. 2015;11(7):e1005008-e.
37. Jia W, Rajani C, Xu H, Zheng X. Gut microbiota alterations are distinct for primary colorectal cancer and hepatocellular carcinoma. Protein Cell. 2021;12(5):374-93.
38. Hu Y, Le Leu RK, Christophersen CT, Somashekar R, Conlon MA, Meng XQ, et al. Manipulation of the gut microbiota using resistant starch is associated with protection against colitis-associated colorectal cancer in rats. Carcinogenesis. 2016;37(4):366-75.
39. Kemis JH, Linke V, Barrett KL, Boehm FJ, Traeger LL, Keller MP, et al. Genetic determinants of gut microbiota composition and bile acid profiles in mice. PLoS Genet. 2019;15(8):e1008073.

652 40. Zarrinpar A, Chaix A, Xu ZZ, Chang MW, Marotz CA, Saghatelian A, et al. Antibiotic-
653 induced microbiome depletion alters metabolic homeostasis by affecting gut signaling and
654 colonic metabolism. Nat Commun. 2018;9(1):2872.
655 41. Grosser G, Müller SF, Kirstgen M, Döring B, Geyer J. Substrate Specificities and
656 Inhibition Pattern of the Solute Carrier Family 10 Members NTCP, ASBT and SOAT. Front Mol
657 Biosci. 2021;8:689757.
658 42. Tian Y, Gui W, Koo I, Smith PB, Allman EL, Nichols RG, et al. The microbiome
659 modulating activity of bile acids. Gut microbes. 2020;11(4):979-96.
660 43. Ju T, Kong JY, Stothard P, Willing BP. Defining the role of Parasutterella, a previously
661 uncharacterized member of the core gut microbiota. ISME J. 2019;13(6):1520-34.
662 44. Devlin AS, Fischbach MA. A biosynthetic pathway for a prominent class of
663 microbiota-derived bile acids. Nat Chem Biol. 2015;11(9):685-90.
664 45. Liu HX, Rocha CS, Dandekar S, Wan YJ. Functional analysis of the relationship
665 between intestinal microbiota and the expression of hepatic genes and pathways during the
666 course of liver regeneration. J Hepatol. 2016;64(3):641-50.
667 46. He T, Cheng X, Xing C. The gut microbial diversity of colon cancer patients and the
668 clinical significance. Bioengineered. 2021;12(1):7046-60.
669 47. Bailey AM, Zhan L, Maru D, Shureiqi I, Pickering CR, Kiriakova G, et al. FXR silencing
670 in human colon cancer by DNA methylation and KRAS signaling. Am J Physiol Gastrointest
671 Liver Physiol. 2014;306(1):G48-G58.
672 48. Fu T, Coulter S, Yoshihara E, Oh TG, Fang S, Cayabyab F, et al. FXR Regulates Intestinal
673 Cancer Stem Cell Proliferation. Cell. 2019;176(5):1098-112.e18.
674 49. Hagi T, Geerlings SY, Nijsse B, Belzer C. The effect of bile acids on the growth and
675 global gene expression profiles in Akkermansia muciniphila. Applied Microbiology and
676 Biotechnology. 2020;104(24):10641-53.
677 50. Ovadia C, Perdones-Montero A, Spagou K, Smith A, Sarafian MH, Gomez-Romero M,
678 et al. Enhanced Microbial Bile Acid Deconjugation and Impaired Ileal Uptake in Pregnancy
679 Repress Intestinal Regulation of Bile Acid Synthesis. Hepatology. 2019;70(1):276-93.
680 51. Theriot CM, Bowman AA, Young VB. Antibiotic-Induced Alterations of the Gut
681 Microbiota Alter Secondary Bile Acid Production and Allow for Clostridium difficile Spore
682 Germination and Outgrowth in the Large Intestine. mSphere. 2016;1(1).
683 52. Wei W, Wang H-F, Zhang Y, Zhang Y-L, Niu B-Y, Yao S-K. Altered metabolism of bile
684 acids correlates with clinical parameters and the gut microbiota in patients with diarrhea-
685 predominant irritable bowel syndrome. World J Gastroenterol. 2020;26(45):7153-72.
686 53. Palm NW, de Zoete MR, Cullen TW, Barry NA, Stefanowski J, Hao L, et al.
687 Immunoglobulin A coating identifies colitogenic bacteria in inflammatory bowel disease. Cell.
688 2014;158(5):1000-10.
689 54. Miyauchi E, Kim SW, Suda W, Kawasumi M, Onawa S, Taguchi-Atarashi N, et al. Gut
690 microorganisms act together to exacerbate inflammation in spinal cords. Nature.
691 2020;585(7823):102-6.
692 55. Umar S. Citrobacter Infection and Wnt signaling. Curr Colorectal Cancer Rep.
693 2012;8(4).
694 56. da Silva Duarte V, Dos Santos Cruz BC, Tarrah A, Sousa Dias R, de Paula Dias Moreira
695 L, Lemos Junior WJF, et al. Chemoprevention of DMH-Induced Early Colon Carcinogenesis in
696 Male BALB/c Mice by Administration of Lactobacillus Paracasei DTA81. Microorganisms.
697 2020;8(12).
698 57. Zeng H, Ishaq SL, Liu Z, Bukowski MR. Colonic aberrant crypt formation accompanies
699 an increase of opportunistic pathogenic bacteria in C57BL/6 mice fed a high-fat diet. J Nutr
700 Biochem. 2018;54:18-27.
701 58. Zhang W, An Y, Qin X, Wu X, Wang X, Hou H, et al. Gut Microbiota-Derived
702 Metabolites in Colorectal Cancer: The Bad and the Challenges. Front Oncol. 2021;11:739648.

59. Wang X, Huycke MM. Extracellular superoxide production by Enterococcus faecalis promotes chromosomal instability in mammalian cells. Gastroenterology. 2007;132(2):551-61.
60. Liu Y, Zhang S, Zhou W, Hu D, Xu H, Ji G. Secondary Bile Acids and Tumorigenesis in Colorectal Cancer. Front Oncol. 2022;12:813745.
61. Peters BA, Dominianni C, Shapiro JA, Church TR, Wu J, Miller G, et al. The gut microbiota in conventional and serrated precursors of colorectal cancer. Microbiome. 2016;4(1):69.
62. Rosshart SP, Vassallo BG, Angeletti D, Hutchinson DS, Morgan AP, Takeda K, et al. Wild Mouse Gut Microbiota Promotes Host Fitness and Improves Disease Resistance. Cell. 2017;171(5):1015-28.e13.
63. Leystra AA, Clapper ML. Gut Microbiota Influences Experimental Outcomes in Mouse Models of Colorectal Cancer. Genes (Basel). 2019;10(11).
64. Wu Y, Jiao N, Zhu R, Zhang Y, Wu D, Wang AJ, et al. Identification of microbial markers across populations in early detection of colorectal cancer. Nat Commun. 2021;12(1):3063.
65. Zhang YK, Zhang Q, Wang YL, Zhang WY, Hu HQ, Wu HY, et al. A Comparison Study of Age and Colorectal Cancer-Related Gut Bacteria. Front Cell Infect Microbiol. 2021;11:606490.
66. Lavelle A, Nancey S, Reimund JM, Laharie D, Marteau P, Treton X, et al. Fecal microbiota and bile acids in IBD patients undergoing screening for colorectal cancer. Gut microbes. 2022;14(1):2078620.
67. Geller LT, Barzily-Rokni M, Danino T, Jonas OH, Shental N, Nejman D, et al. Potential role of intratumor bacteria in mediating tumor resistance to the chemotherapeutic drug gemcitabine. Science. 2017;357(6356):1156-60.

730 **Figure Legends**

731 **Figure 1. Alpha (α) and beta (β) diversity are altered across time in mice treated with either**
732 **PBS or AOM.** Faecal samples were collected throughout the experiment and analysed by 16S
733 rRNA gene sequencing 8-, 12-, 24-, and 48-weeks following administration of either PBS or
734 AOM. α-diversity was measured using Shannon, Observed Species and Phylogenetic Diversity
735 (PD) *p<0.05 after FDR correction. Data are presented as median (IQR) (a). PERMANOVA of
736 unweighted Unifrac distances were used to examine the β-diversity visualised by principal
737 coordinate analysis (b). n=7-8 per group.

738 **Figure 2. Histograms of the community composition of gut microbiota at the phylum level**
739 **and co-abundance groups (CAG).** The impact of AOM on the major phyla in faecal samples
740 of mice at 8-, 12-, 24-, and 48-weeks following administration of either PBS or AOM (a). Each
741 bar chart represents the average reads of the group (n=7–8). Each phylum is expressed as a
742 percentage of the total number of reads for the particular group. Species with a relative
743 abundance of less than 1% were classified as unassigned. Bar charts showing the proportion
744 of specific CAGs detected in AOM and PBS treated groups (b). Seven CAGs were identified
745 and PERMANOVA determined that all CAGs were significantly different (p<0.05 after FDR
746 adjustment). n=7-8.

747 **Figure 3. Taxa which differed significantly in their abundance between groups.** From the
748 data acquired by 16S RNA gene sequencing, operational taxonomic units were clustered
749 based on 97% sequence similarity and taxonomy was assigned using BLAST against the SILVA
750 SSURef data base. Only significantly different taxa are presented here. Data are presented as
751 the z-scores of the abundances scaled by row. Taxa highlighted in red font represent taxa
752 that were altered at two or more time-points. n=7-8 per group. *p<0.05, **p<0.01,
753 ***p<0.001 after FDR adjustment.

754 **Figure 4. Alterations in faecal bile acid profiles and transporter gene expression between**
755 **AOM and PBS treated mice.** Bile acids (a, c-f) were measured by UPLC-MS from mice at 8-,
756 12-, 24-, and 48-weeks and ASBT (b) was measured by qRT-PCR following administration of
757 either PBS or AOM. Faecal bile acid levels are presented as absolute values. Data are
758 presented as mean ± SEM. n=7-8 per group. *p<0.05, **p<0.01, ***p<0.001.

759 **Figure 5. Alterations in immunoregulatory gene expression between AOM and PBS treated**
760 **mice**. Cytokines and chemokines were measured by qRT-PCR from mice at 8-, 12-, 24-, and
761 48-weeks following administration of either PBS or AOM. n=7-8 except for samples where
762 the values were below the detection threshold (a). HT29 cells were stimulated for four hours
763 with faecal waters derived from PBS- or AOM-treated mice (1:10 dilution) and changes in

764 gene expression measured by qRT-PCR (n=3) (b). The heat maps depict fold change in gene
765 expression. *p<0.05, **p<0.01, ***p<0.001 after FDR correction. White box in panel (a)
766 depicts gene expression that was greater than the fold change range for the other genes but
767 was not significantly different between treatment groups.

a. Alpha Diversity

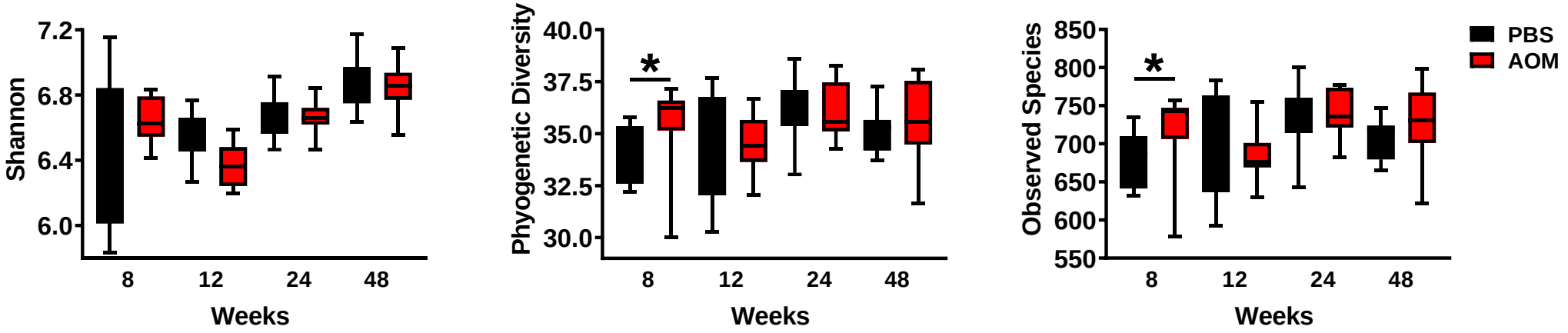

b. Beta Diversity

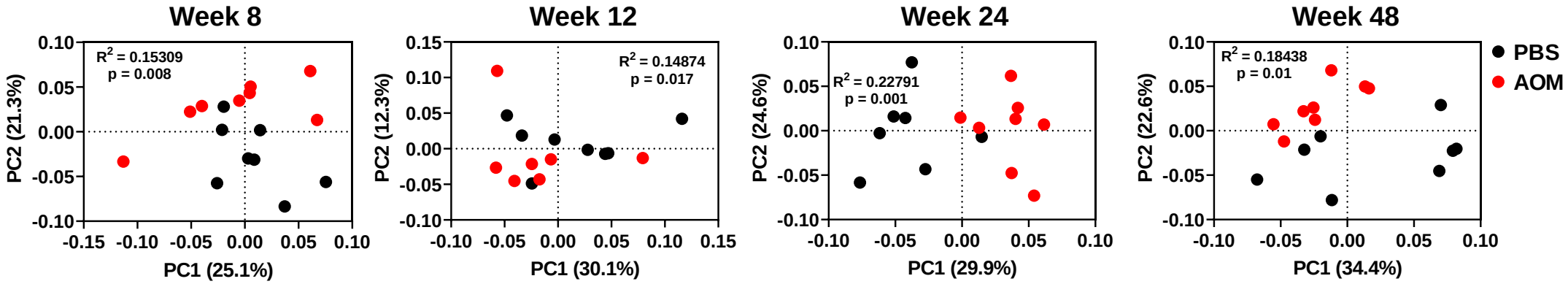

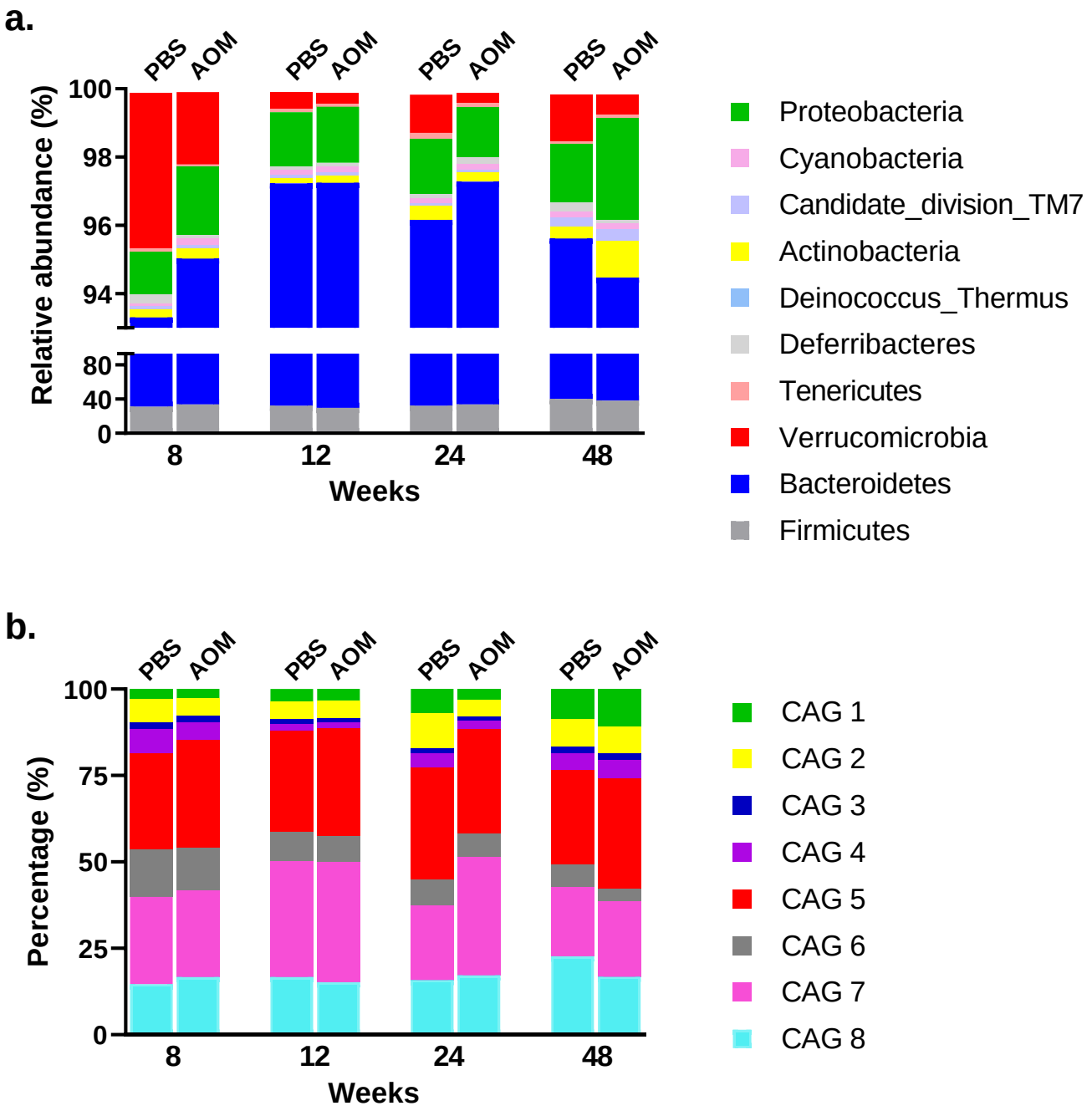
a.
PBS
AOM
Relative abundance (%)
100
98
96
94
80
40
0
8
12
24
48
Weeks
Proteobacteria
Cyanobacteria
Candidate_division_TM7
Actinobacteria
Deinococcus_Thermus
Deferribacteres
Tenericutes
Verrucomicrobia
Bacteroidetes
Firmicutes
b.
PBS
AOM
Percentage (%)
100
75
50
25
0
8
12
24
48
Weeks
CAG 1
CAG 2
CAG 3
CAG 4
CAG 5
CAG 6
CAG 7
CAG 8

a. week 8

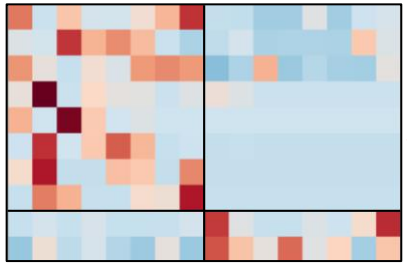

Parvibacter**
Lactobacillus*
Christensenella**
Clostridium sensu strictu 1*
Marvinbryantia*
Turicibacter***
Psychrobacter*
Vibrio*
Olsenella*
Clostridiales vadinBB60; uncultured rumen bacterium*

b. week 12

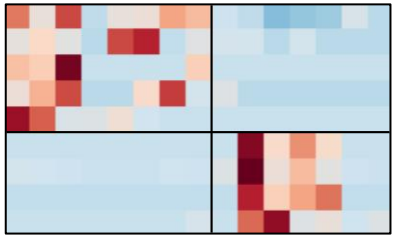

Bacterioidales S24-7; uncultured organism**
Lachnospira*
Psychrobacter*
Vibrio*
Mollicutes RF9; Firmicutes bacterium CAG:822**
Gordonibacter*
Clostridium sensu stricto 1*
Anaerofilum*
Mollicutes RF9; uncultured rumen bacterium**

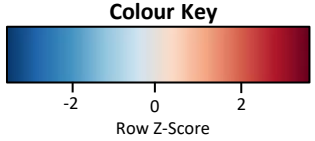

c. week 24

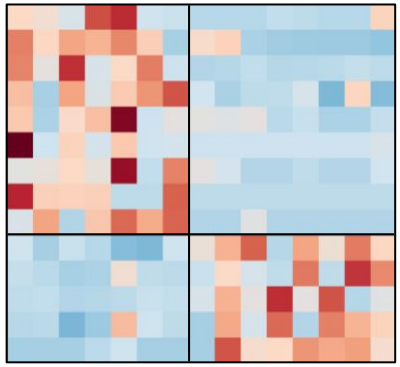

Porphyromonadaceae; uncultured**
Rikenella**
Bacterioidales S24-7; mouse gut metagenome***
Bacterioidales S24-7; uncultured organism*
Enterococcus*
Marvinbryantia**
Escherichia-Shigella**
Psychrobacter**
Vibrio**
Rikenellaceae RC9 gut group**
Caldicoprobacter*
Oscillibacter*
Ruminococcaceae; uncultured*
Mollicutes RF9; uncultured rumen bacterium**

d. week 48

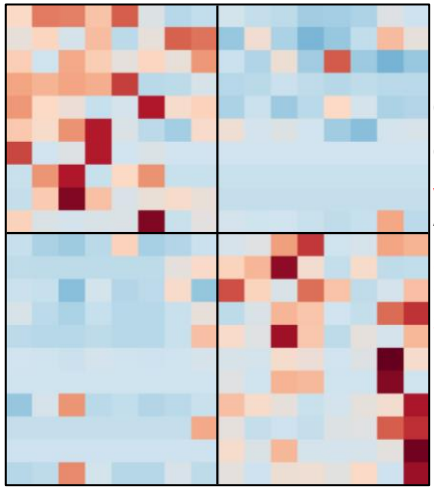

Bacterioidales S24-7; mouse gut metagenome*
Bacterioidales S24-7; uncultured Bacterioidales bacterium*
Defluvitaleaceae; uncultured *
Marvinbryantia*
Oscillibacter*
Defltia*
Citrobacter*
Psychrobacter*
Vibrio**
Akkermansia*
Bifidobacterium*
Clostridium sensu stricto**
Clostridiales vadinBB60; uncultured rumen bacterium**
Allobaculum*
Turicibacter*
Parasutterella**
Mollicutes RF9; Firmicutes bacterium CAG:822*
Mollicutes RF9; uncultured bacterium*
Mollicutes RF9; uncultured Mollicutes bacterium*
Mollicutes RF9; uncultured rumen bacterium***
Mollicutes RF9; unidentified*

a. Total bile acids

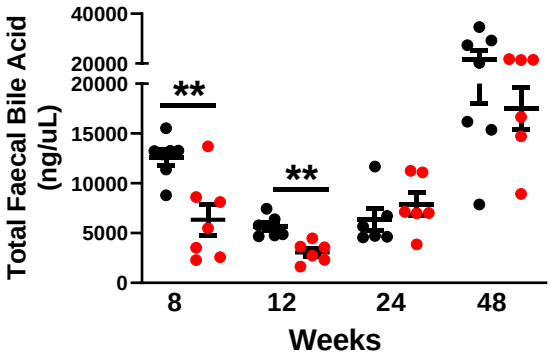

b. Colonic *ASBT* gene expression

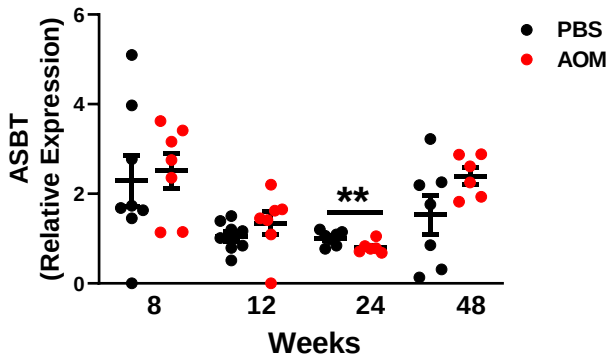

c. week 8

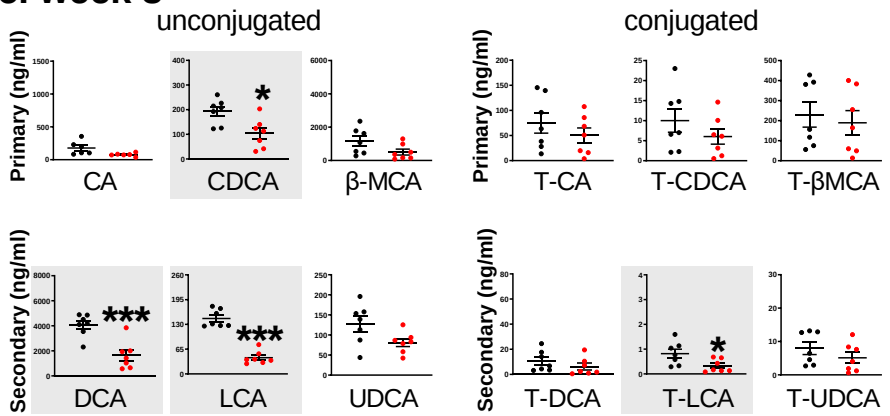

d. week 12

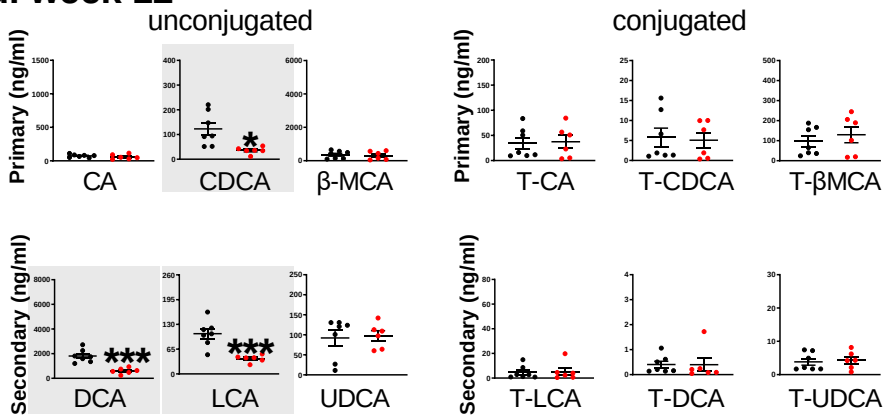

e. week 24

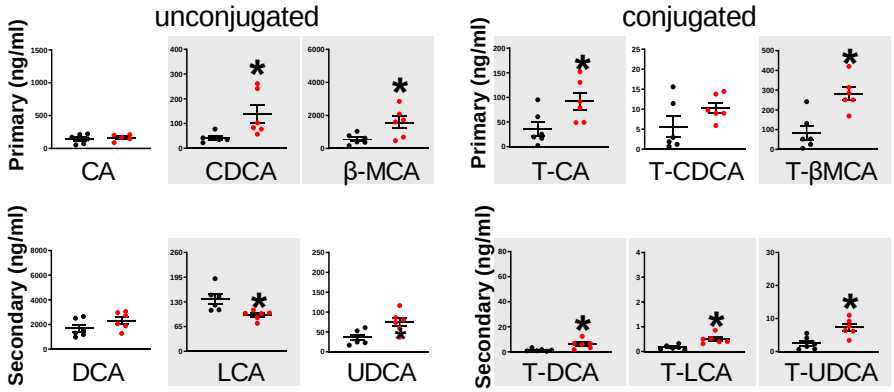

f. week 48

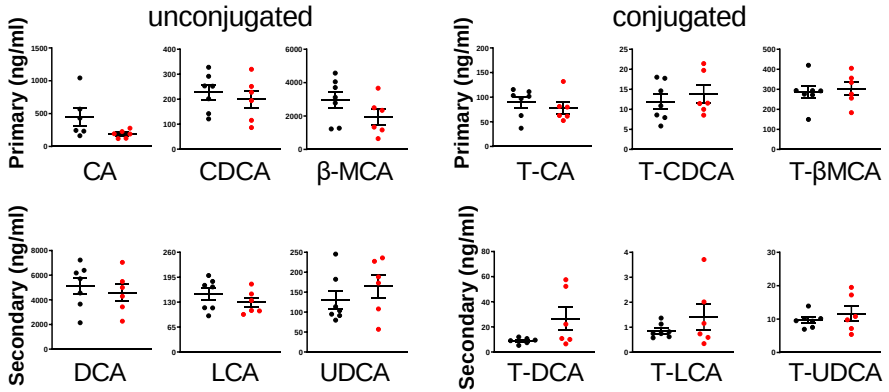

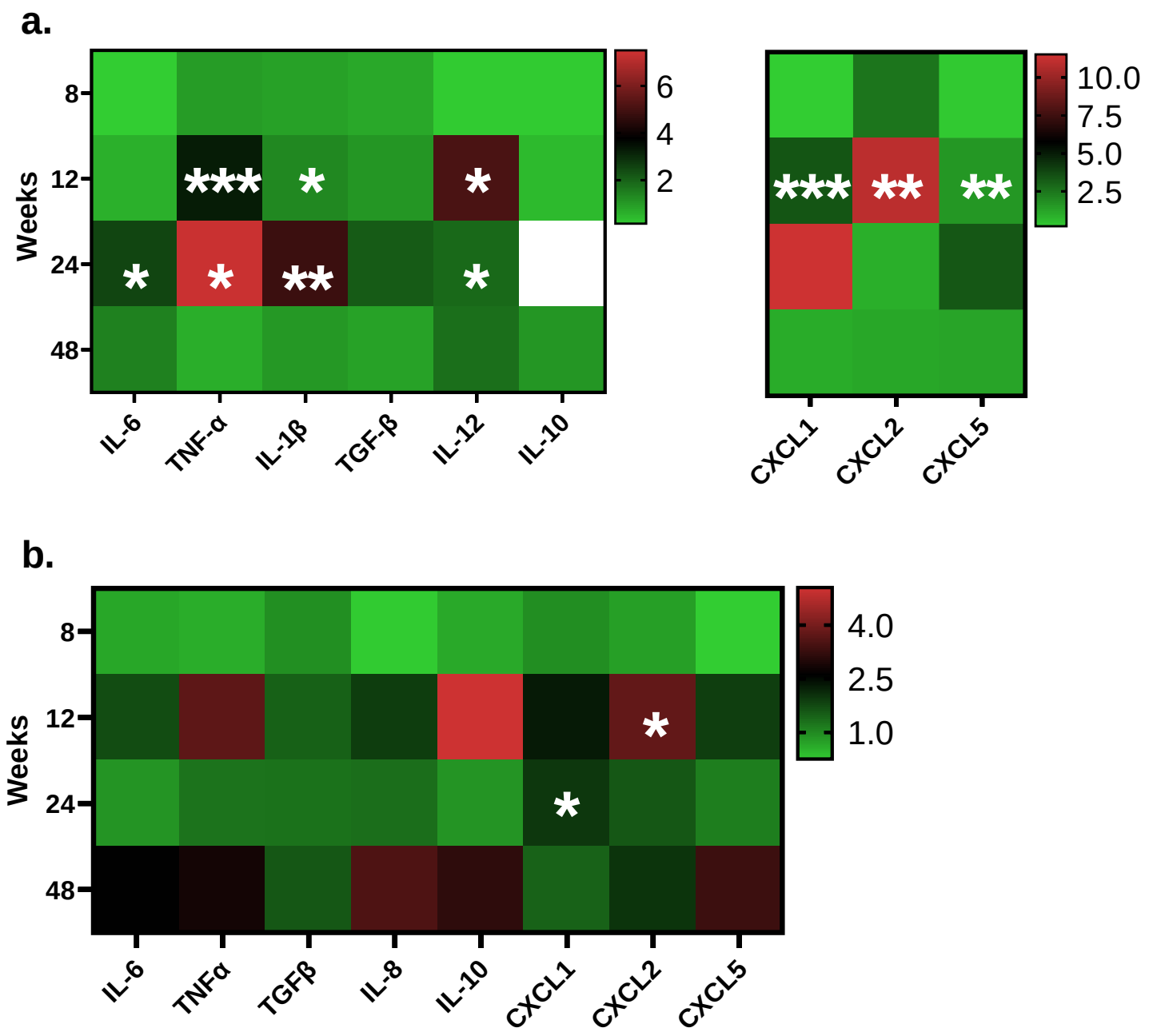
a.
Weeks
8
12
24
48
IL-6
TNF-α
IL-1β
TGF-β
IL-12
IL-10
6
4
2
CXCL1
CXCL2
CXCL5
10.0
7.5
5.0
2.5
b.
Weeks
8
12
24
48
IL-6
TNFα
TGFβ
IL-8
IL-10
CXCL1
CXCL2
CXCL5
4.0
2.5
1.0

49 Spadina Ave. Suite 200
Toronto ON M5V 2J1 Canada
www.biorender.com

Confirmation of Publication and Licensing Rights

November 18th, 2022
Science Suite Inc.

Subscription:	*Individual*
Agreement number:	*DB24NUZQPD*
Journal name:	*British Journal of Cancer*

To whom this may concern,

This document is to confirm that Aileen Houston has been granted a license to use the BioRender content, including icons, templates and other original artwork, appearing in the attached completed graphic pursuant to BioRender's Academic License Terms. This license permits BioRender content to be sublicensed for use in journal publications.

All rights and ownership of BioRender content are reserved by BioRender. All completed graphics must be accompanied by the following citation: "Created with BioRender.com".

BioRender content included in the completed graphic is not licensed for any commercial uses beyond publication in a journal. For any commercial use of this figure, users may, if allowed, recreate it in BioRender under an Industry BioRender Plan.

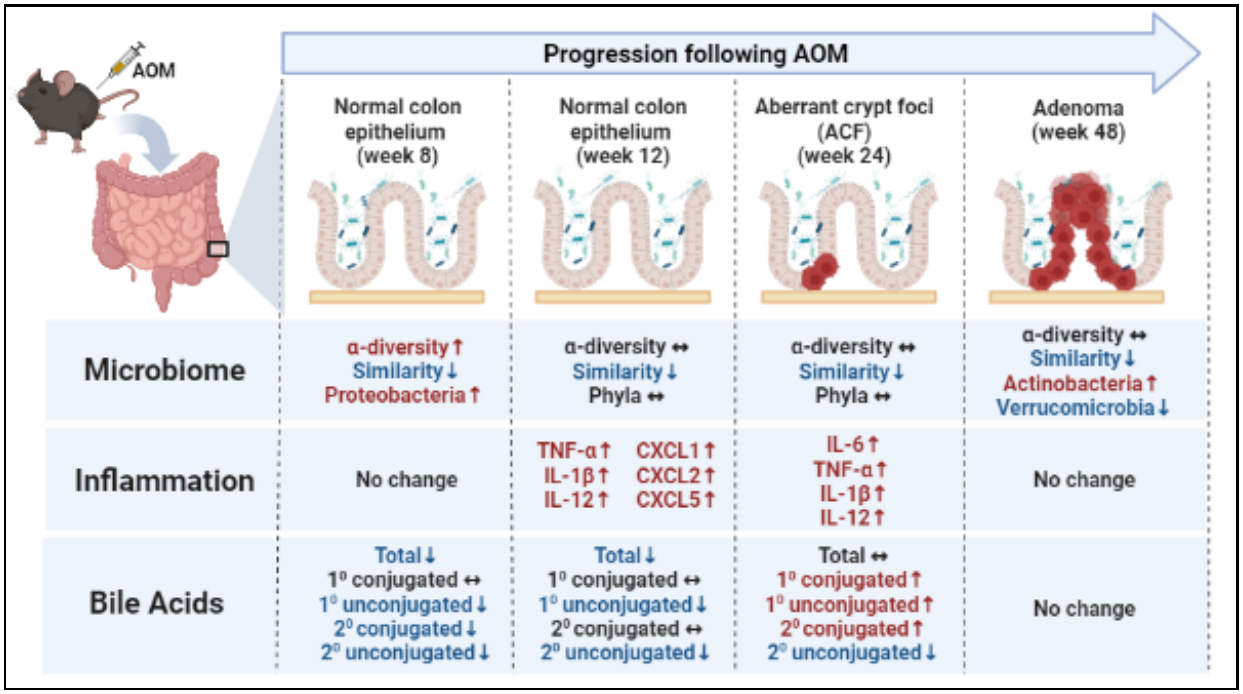

For any questions regarding this document, or other questions about publishing with BioRender refer to our BioRender Publication Guide, or contact BioRender Support at support@biorender.com.